Е. Бойко, асп.
Киевский национальный університет имени Тараса Шевченко, УНИ "Институт геологии",
ул. Васильковская, 90, г. Киев, 03022, Украина,
E-mail: boyko_ekateruna@ukr.net

МЕТОДИКА ОЦЕНКИ РИСКА ВОЗНИКНОВЕНИЯ НОВЕЙШИХ ОПОЛЗНЕЙ ЮГО-ЗАПАДНОГО БЕРЕГА КРЫМА

Инженерно-геологическое освоение территории южного берега Крыма, который является активной геолого-тектонической структурой, всегда усложнялось широким распространением экзогенных геологических процессов (ЭГП). Особенно опасным явлением для региона являются оползни. Практика укрепления склонов и устранения основных факторов оползнеобразования на исследуемой территории продолжается почти полстолетия. За указанный период разработан комплекс методик с целью осуществления инженерно-геологических мероприятий, а также внедрены основы прогнозирования активизации оползней и их обнаружения на местности. Однако, несмотря на укрепление контрфорсов и стабилизацию грандиозных оползневых систем, на сегодняшний день наблюдается тенденция активизации и возникновения современных оползней неглубокого заложения техногенного и эрозионного происхождения. Последние формируются в покровных элювиально-делювиальных отложениях, которые залегают на флишевых формациях таврической серии и среднеюрского возраста. Повсеместное распространение небольших и неглубоких оползней создает проблему их выявления во время мониторинговых работ. Методы пространственного моделирования оползнеопасных территорий ("геодинамического" или "оползневого" потенциала), которые базируются на теории вероятности, разработаны на примере отдельных оползневых районов, поэтому нуждаются в использовании детализированной информации на основе крупномасштабных съёмок. С другой стороны, оценка предрасположенности территории к развитию оползней с использованием расчётных показателей – коэффициента линейного и площадного поражения – не отображает динамики и направления развития процесса. Таким образом, необходимость оценки риска активизации и образования современных оползней нуждается в создании более приемлемого с точки зрения указанных критериев – информативности и надёжности, метода регионального пространственного анализа развития процесса. Предложенная в исследовании методика учитывает как активность (динамику развития) оползней в пределах региона, так и интенсивность их проявлений (площадное поражение). Впервые с целью обоснования распределения коэффициента риска в пределах юго-западного побережья Крыма была присвоена количественная характеристика критерию генетического типа вмещающих пород с использованием историко-геологического метода Г.С. Золотарёва. В результате исследования была составлена карта районирования исследуемой территории по степени риска проявления оползней неглубокого залегания. Построенная модель отображает как направление оползнеобразования, так и состояние геологической среды. Карта оценки риска распространения оползней в комплексе с картой техногенной нагрузки являются информативной основой районирования территории по степени устойчивости геологической среды к разным типам техногенных воздействий, а также к развитию оползней неглубокого заложения.

Ключевые слова: риск, оползень в покровных породах, активность, поражение, устойчивость склона.

ГЕОЛОГІЧНА ІНФОРМАТИКА

UDC 550.344

D. Malytskyy, Dr. Sci. (Phys.-Math.), Prof.
E-mail: dmytro@cb-igph.lviv.ua,
O. Muyla, Cand. Sci. (Phys.-Math.), Research Associate
E-mail: orestaro@gmail.com,
O. Hrytsaj, Postgraduate Student
E-mail: grycaj.oksana@gmail.com,
O. Kutniv, Engineer
E-mail: okutniv@yahoo.com,
O. Obidina, Postgraduate Student
E-mail: jane.det@yandex.ua,
Carpathian Branch of
Subbotin Institute of Geophysics NAS of Ukraine
3-b Naukova Str., Lviv, Ukraine 79060

MOMENT TENSOR INVERSION OF WAVE FORMS

(Рекомендовано членом редакційної колегії д-ром фіз.-мат. наук, проф. Б.П. Масловим)

The authors present a moment tensor inversion of waveforms, which is more robust and yields more stable and more accurate results than standard approaches. The inversion is solved in two steps. First, a point source of seismic waves is considered, with defined location and origin time. Matrix method is used to solve the problem of wave propagation in the medium modeled as a horizontally layered heterogeneous elastic structure (isotropic and/or anisotropic). In order to allow the source mechanism to change with time each moment tensor component has its own time history. The source is described by the full moment tensor M_{lm} A numerical technique developed based on forward modeling is used for the inversion of the observed waveforms for the components of moment tensor and the earthquake source-time function (STF(t)). The method provides a good estimate for the complete mechanism when records are treated, which corresponds to a velocity model contained inside the interpolation range. The method of waveform inversion using only direct P- and S-waves at stations that we have developed allows us to retrieve the moment tensor of a point source as a function of time. We computed the moment tensor solutions also using the graphic method. The traditional graphical method is based on the P-waves prior arrival using information about fuzzy first motion and the S/P amplitude ratio. The polarities between P-waves first motion were defined from complete records on seismograms taking into account the possible inversion of the sign on the z-component. A logarithm of the S/P amplitude ratio is calculated using seismic data received at each station from the three components. Input data for the azimuth and take-off angle are calculated by software packages for each event. Finally, the proposed moment tensor inversion is tested on real data for the earthquakes of 24.04.2011 ($13^h02^m12^s$, 35.92°N, 14.95°E (near Malta), M_w4.0) and 29.12.2013 ($17^h09^m0.04^s$, 41.37°N, 14.45°E (Southern Italy), M_w4.9).

Keywords: matrix method, moment time function, earthquake mechanism, tensor of seismic moment.

Introduction. The basis for quantifying the earthquake sources is seismic moment tensor. The moment tensor is calculated by several approaches: using amplitudes of seismic waves [2, 11], S/P amplitude ratios [3, 8], full waveforms [1, 4, 6, 9, 10]. The inversion of full waveforms is a widely used approach applicable on all scales: from small to large earthquakes. It is usually applied employing the point-source approximation and assuming a time independent focal mechanism. The inversion is performed in the time domain or in the frequency domain. The inversion yields seismic moment tensor and, as a result, source time function, $STF(t)$. The waveform inversion is a datademanding procedure: it needs a good knowledge of the velocity model, an accurate source location and good azimuthal coverage of the focal sphere. The wave form inversion is a non-linear procedure. In this paper, authors propose a new inversion scheme for computing the time-independent moment tensors. The proposed inversion is performed in two steps. First, authors consider propagation of seismic waves in vertically inhomogeneous media and develop a version of matrix method for calculation of synthetic seismograms on the upper surface of the layered isotropic and/or anisotropic medium. The point source is located inside a layer and is represented with seismic moment tensor. The results for the field of displacements on the upper surface are presented in a matrix form using amplitude spectra, and separately for the far-field and the near field. Subsequently, only the far-field displacements are considered. Second, the moment time functions $M_{lm}(w)$ are calculated based on generalized inversion and transformed into $M_{lm}(t)$ by applying the inverse Fourier transform and factorized in seismic moment tensor M_{lm} and $STF(t)$: $M_{lm}(t) = M_{lm}STF(t)$. The factorization means that the focal mechanism is independent of time. Here it should be noted that analytic-numeric approaches to determination of seismic moment tensor have been formulated with application of eigenvector analysis reducing the problem to system of linear equations. The assumption of time-independent focal mechanism is a very good approximation while studying the mechanisms in the frequency range of direct P- and S-waves. The factorization yields both the source time function $STF(t)$ and the seismic moment tensor M_{lm}. Therefore, based on the matrix method of Thomson and Haskell, the authors develop a new analytical technique for calculation of seismic waves in layered (isotropic and/or anisotropic) media. They present an approach to determination of the source time function and the seismic moment tensor from the observed waveforms. The goal of this paper is to obtain the focal mechanism using waveform inversion for moment time functions at one station. Versions of focal mechanisms of two earthquakes: near Malta and Southern Italy obtained alternatively by graphic method and by waveform inversion are shown in Fig. 1 and Fig. 2. It also should be noted that choice of velocity model is very important in determining the focal mechanisms.

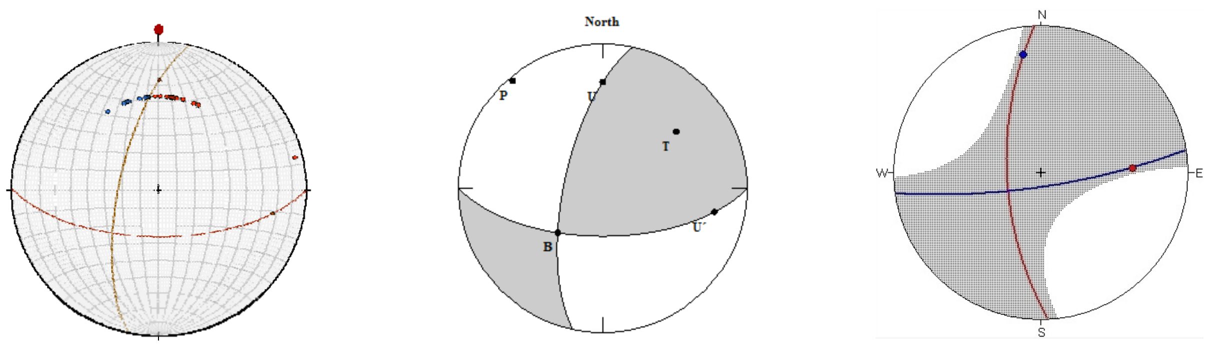

a b c

Fig. 1. The lower hemisphere equal area projections of focal mechanisms obtained by graphic method (a, b) and by waveform inversion for moment time functions (c) from the first peaks of $M_{lm}(t)$ functions shown in Fig. 3

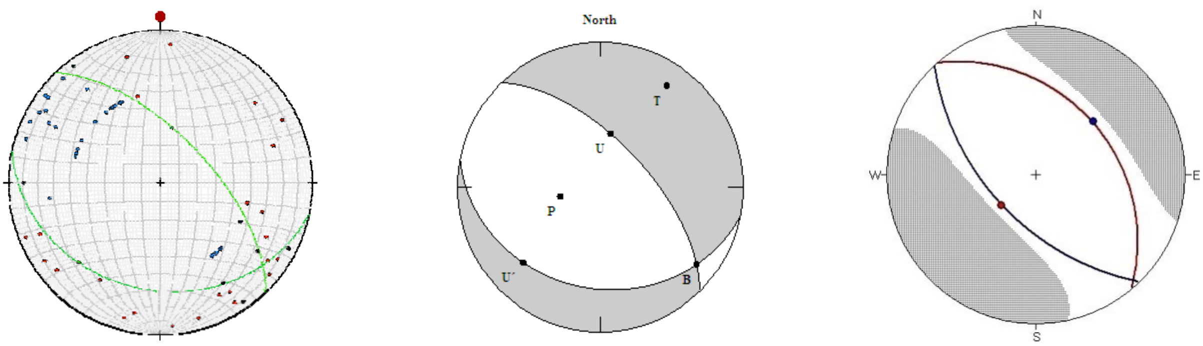

a b c

Fig. 2. Lower hemisphere equal area projections of focal mechanisms obtained by graphic method (a, b) and by the waveform inversion for moment time functions (c) from the first peaks of $M_{lm}(t)$ functions shown in Fig. 4

1. Frequency-domain waveform inversion for a moment time function. In the time domain and in cylindrical coordinates (r,ϕ,z), the following expressions have been obtained, using the matrix method, in [5] for the far-field displacements on the upper surface of layered medium for a point source:

$$\begin{pmatrix} u_z^{(0)} \\ u_r^{(0)} \end{pmatrix} = \sum_{i=1}^{3} \int_0^{\infty} k^2 I_i L^{-1}[M_i \mathrm{g_i}]\,dk ,$$

$$u_{\phi}^{(0)} = \sum_{i=5}^{6} \int_0^{\infty} k^2 J_i L^{-1}\left[M_i \mathrm{g}_{\mathrm{i}\phi}\right] dk \qquad (1)$$

$$I_1 = \begin{pmatrix} J_1 & 0 \\ 0 & J_0 \end{pmatrix},\ I_2 = \begin{pmatrix} J_0 & 0 \\ 0 & J_1 \end{pmatrix},\ I_3 = I_2 .\ J_5 = J_0 ,\ J_6 = J_1$$

where J_0 and J_1 are Bessel functions, k – horizontal wave number, $L^{-1}[k\eta]$ – inverse Laplace transform, η – coefficient of Mellin, and quantity M_i contains the six moment time functions.

Eq. (1) can be expressed in matrix form for direct P- and S-waves at N stations ($i=1,\ldots,N$) in the spectral domain:

$$\begin{aligned}\mathbf{K}_1\mathbf{M} &= \mathbf{U}^{(0)}_{\mathbf{S}1}\\ \mathbf{K}_2\mathbf{M} &= \mathbf{U}^{(0)}_{\mathbf{S}2}\\ &\ldots\\ \mathbf{K}_N\mathbf{M} &= \mathbf{U}^{(0)}_{\mathbf{S}N}\end{aligned} \tag{2}$$

where

$$\mathbf{M} = \left(M_{xz}(w),\ M_{yz}(w),\ M_{zz}(w),\ M_{xx}(w),\ M_{yy}(w),\ M_{xy}(w)\right)^T = M_{lm}(w)$$

$$\mathbf{K}_\mathrm{i} = \begin{pmatrix} K^P_{11} & K^P_{12} & K^P_{13} & K^P_{14} & K^P_{15} & K^P_{16}\\ K^s_{21} & K^s_{22} & K^s_{23} & K^s_{24} & K^s_{25} & K^s_{26}\\ K^P_{31} & K^P_{32} & K^P_{33} & K^P_{34} & K^P_{35} & K^P_{36}\\ K^s_{41} & K^s_{42} & K^s_{43} & K^s_{44} & K^s_{45} & K^s_{46}\\ K^P_{51} & K^P_{52} & K^P_{53} & K^P_{54} & K^P_{55} & K^P_{56}\\ K^s_{61} & K^s_{62} & K^s_{63} & K^s_{64} & K^s_{65} & K^s_{66}\end{pmatrix}$$ – the matrix of velocity model at *i* station.

Each vector in $\left(U^{(0)}_{S1}, U^{(0)}_{S1}, \ldots U^{(0)}_{SN}\right)^T$ contains six displacement components of direct P- and S-waves at N stations (*i=1,…,N*).

$$\mathbf{GM} = \mathbf{U}^{(0)}_{\mathbf{S}},\quad \mathbf{G} = \begin{pmatrix}\mathbf{K}_1\\ \vdots\\ \mathbf{K}_N\end{pmatrix} \tag{3}$$

Matrix **K** and vector **M** and $\mathbf{U}^{(0)}_{\mathbf{S}}$ are functions of frequency. The vector **M** of moment time functions is obtained using the generalized inversion:

$$\tilde{\mathbf{G}}^*\mathbf{GM} = \tilde{\mathbf{G}}^*\mathbf{U}^{(0)}_{\mathbf{S}} \tag{4}$$

$$\mathbf{M} = (\tilde{\mathbf{G}}^*\mathbf{G})^{-1}\tilde{\mathbf{G}}^*\mathbf{U}^{(0)}_{\mathbf{S}}, \tag{5}$$

where $(\tilde{\mathbf{G}}^*\mathbf{G})^{-1}\tilde{\mathbf{G}}^*$ is the generalized inverse of **G**. Eq.(5) is solved at each frequency. The moment time functions $M_{lm}(w)$ are calculated using Eq. (5) and can be transformed into $M_{lm}(t)$ by applying the inverse Fourier transform and can be written as follows:

$$M_{lm}(t) = M_{lm}STF(t), \tag{6}$$

where M_{lm} is the seismic moment tensor and $STF(t)$ is the source time function.

The factorization means that the focal mechanism is independent of time. Although the focal mechanism may be dependent on the frequency range of the studied waves [11] the assumption of time independent focal mechanism is a very good approximation while determining it in the frequency range of direct P- and S-waves. It should be noted that the results of determination of moment time function (5) can be obtained also using seismic data at only one station.

2. Numerical modeling. In this section, the efficiency of the proposed inversion is tested numerically on two events and compared with other standard methods. The problem of determination of the focal mechanism solutions for the earthquakes in the regions where local seismic activity is low has recently become especially important. Particularly it is so in the Carpathian region of Ukraine, where insufficient number of stations combines with low seismic activity. For determination of focal mechanisms a traditional graphical method is proposed, utilizing the polarities of first arrivals of P-waves and accounting for the information on fuzzy polarities by estimating the *S*/*P* amplitude ratios in them [7]. In the current paper, the determination of focal mechanisms is described for the earthquakes of 24.04.2011 ($13^h02^m12^s$, 35.92°N, 14.95°E (near Malta), M_w4.0) and 29.12.2013 (17^h09^m0.04, 41.37°N, 14.45°E (southern Italy), M_w4.9) using both the frequency-domain waveform inversion for moment time functions and the graphical method. The focal mechanisms are obtained for these events by graphical method according to the input data (Tab. 1 and Tab. 2) and velocity models (Fig. 5a, 5b). The data on first motions of P-waves are plotted upon a lower-hemisphere stereographic projection (Fig. 1, 2) for the two events. The focal mechanisms and the time history are given by the six independent time functions corresponding to the six moment tensor components (indicated in all plots as M_{xz}, M_{xy}, see Fig. 3 and Fig. 4). The focal mechanism solutions obtained by waveform inversion for the moment time functions using the first peaks of $M_{lm}(t)$ functions are not very far from the true mechanisms (see Fig. 1b, 1c and Fig. 2b, 2c). The parameters of focal mechanisms for the events are indicated in Tab. 3 and Tab. 4. The source time duration is 1.2 s for the earthquake of 24.04.2011 and 2.3 s for the earthquake 29.12.2013. It should be noted that the accuracy of velocity model is very important while determining the focal mechanism. In our case, the proposed method gives better results for the moment time function (Fig. 3) and the focal mechanism (Fig. 1) for the event 24.04.2011. Thus, the knowledge of proper structural model plays a crucial role in the inversion of waveforms for the moment tensor and the focal mechanism.

3. Discussions and conclusions. The method of waveform inversion using only direct P- and S-waves at stations that we have developed allows us to retrieve the moment tensor of a point source as a function of time. In comparison with graphic method it has the following advantages:

(1) It allows us to vary the velocity model during inversion.

(2) It allows us to change each vector in $\left(U^{(0)}_{S1}, U^{(0)}_{S1}, \ldots U^{(0)}_{SN}\right)^T$ that contains six displacement components of direct P- and S-waves at N stations (*i=1,…,N*).

The waveform inversion produces moment tensors of varying accuracy. The technique proposed for the moment tensor inversion has been applied to observations of events in Southern Italy and near Malta. The application of the technique to real data indicates that time-frequency approach is robust and produces more reliable moment tensors than other inversion schemes. The inversions, performed with the use of records from time-extended sources, show good resolution of the inverted parameters. The time duration of the sources is retrieved satisfactorily.

In the future papers, the next steps will be considered consisting in development of approaches, based again on matrix method, enabling to model the earthquake rupture, and the inversion for finite-fault source parameters. Extended sources, modeled as a superposition of *N* point sources, will be represented by a number of shear dislocations or double couples with moment tensors. The results for the field of displacements on the upper surface will be presented in matrix form as a sum of displacements from each point source. Equations for the wave fields are essentially similar to ones as for the point source, except for the new amplitude vectors. The vectors would now be frequency, azimuth and the source depth dependent for each point source, reflecting the directivity properties of the composite source. Authors will propose a new approach to determine parameters of a finite-fault source: rupture velocity, slip velocity, rupture time, rise time. Finally, the proposed moment tensor inversion will be tested on real data observed in a complex 3-D inhomogeneous geological environment.

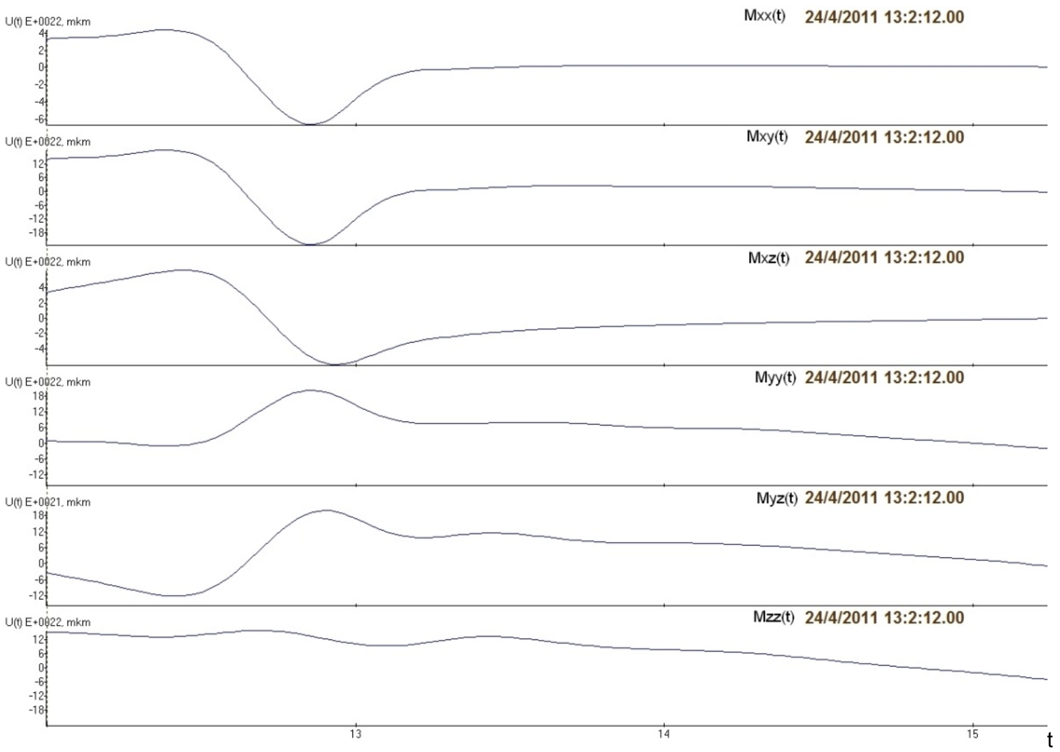

Fig. 3. The time functions $M_{lm}(t)$ corresponding to the six moment tensor components obtained from inversion of the records of the direct P- and S waves at the station WDD for the event of 24.04.2011

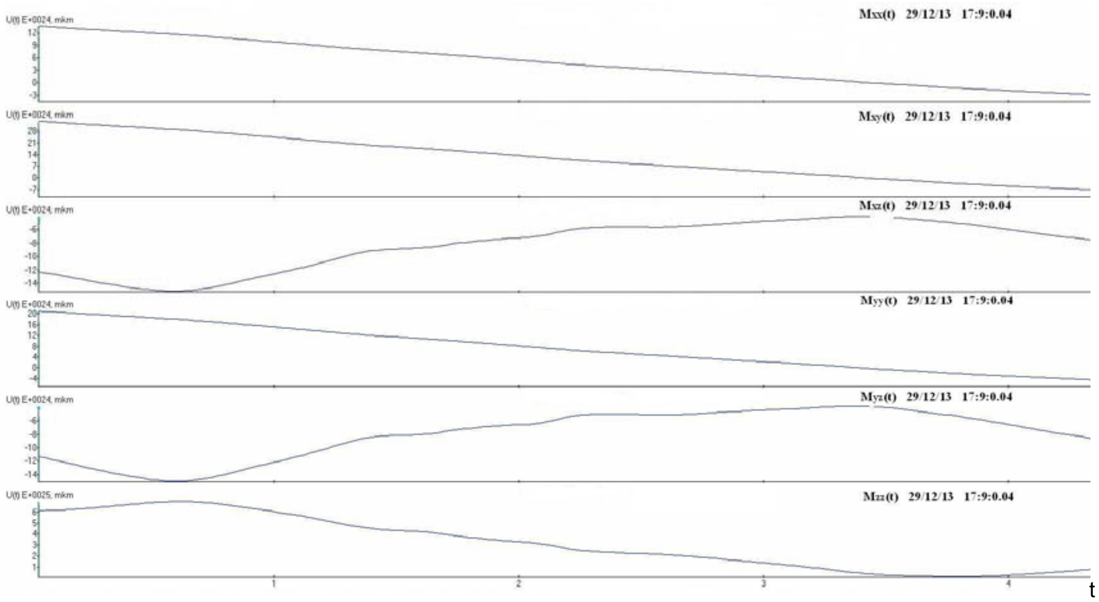

Fig. 4. The time functions $M_{lm}(t)$ corresponding to the six moment tensor components obtained from inversion of the records of the direct P- and S waves at the station PIGN for the event of 29.12.2013

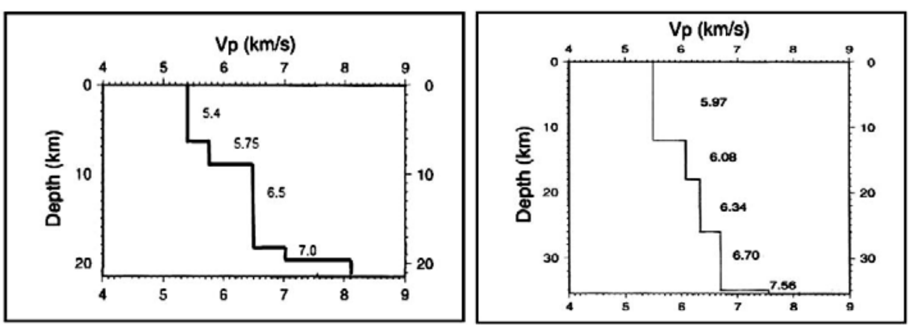

a b

Fig. 5. Velocity models used to compute the focal mechanisms of events of 24.04.2011 (a) and 29.12.2013 (b)

Table 1

The input data for the focal mechanism solution for the event of 24.04.2011

Station	Polarity of first arrival	Epicentral distance, deg	Epicentral distance, km	Azimuth, deg	Incidence angle, deg
WDD	+ iPg	0.355	39.56	256.6	-5.7
HMDC	- iPn	1.05	116.26	352.7	36.6
HAVL	+ iPn	1.05	116.32	7.5	36.6
SSY	+ iPn	1.24	137.72	4.6	36.6
HVZN	- iPn	1.27	141.17	351.6	36.6
HAGA	+ iPn	1.37	152.58	6.8	36.6
RAFF	- iPn	1.39	153.88	340.3	36.6
HLNI	+ iPn	1.43	158.62	357.5	36.6
ECNV	- ePn	1.69	187.21	353.6	36.6
CAGR	- iPn	1.74	193.11	348.2	36.6
ESLN	+ iPn	1.77	196.78	0.6	36.6
RESU	- iPn	1.87	207.57	337.8	36.6
MMME	+ iPn	2.03	225.26	6.8	36.6
GIB	- iPn	2.20	244.02	340.6	36.6
MPAZ	+ iPn	2.20	244.48	22.2	36.6
MPNC	+ iPn	2.25	249.64	8.1	36.6
CORL	- iPn	2.37	263.65	326.8	36.6
MSRU	+ iPn	2.39	264.84	10.6	36.6
IVPL	+ iPn	2.46	272.6	0.6	36.6
ILLI	+ iPn	2.53	280.35	360.0	36.6
JOPP	+ iPn	2.79	309,57	15.2	36.6
PLAC	+ iPn	2.79	310.22	24.7	36.6
CUC	+ iPn	4.13	458.58	9.2	36.6

Table 2

Input data for the focal mechanism solution for the event of 29.12.2013

Station	Polarity of first arrival	Epicentral distance, deg	Epicentral distance, km	Azimuth, deg	Incidence angle, deg
VAGA	+ iPg	.165	18.38	286.4	-31.2
SACR	- iPg	.198	22.06	81.7	-27.0
BSSO	+ iPg	.209	23.28	32.1	-26.1
PIGN	+ iPg	.261	29.08	229.8	-20.4
MIDA	+ iPg	.308	34.27	332.4	-18.4
PSB1	- iPg	.311	35.21	117.8	-17.6
PAOL	+ iPg	.350	38.92	164.7	-16.0
GATE	- iPg	.377	42.83	67.4	-14.6
CERA	+ iPg	.393	43.82	305.7	-14.4
RNI2	+ iPg	.400	44.44	326.9	-15.6
TRIV	+ iPg	.405	45.08	11.2	-13.8
CIGN	+ iPg	.447	49.78	50.2	-12.3
MRB1	- iPg	.464	51.67	121.9	-12.1
MODR	+ iPg	.481	53.6	242.6	-11.4
MOCO	- ePg	.535	59.67	89.7	-11.0
OVO	+ iPg	.543	60.34	183.8	-10.4
MELA	- iPg	.612	68.14	56.4	-8.9
FRES	+ iPg	.627	69.65	15.4	-8.9
POFI	+ iPg	.650	72.37	302.7	-8.9
CAFÉ	- iPg	.686	76.49	119.5	-8.6
LPEL	+ iPg	.705	78.32	344.0	-8.2
SNAL	- iPg	.727	80.92	127.4	-8.0
SGTA	- iPg	.730	81.4	108.4	-8.0
INTR	+ iPg	.759	84.32	328.0	-7.7
VVLD	+ iPg	.793	88.29	309.5	-7.4
MCRV	- iPg	.801	89.06	136.8	-7.5
CAFR	+ iPg	.861	95.68	355.2	-6.4
GUAR	- ePg	.948	105.65	297.0	-6.1
VULT	- iPg	.974	108.54	114.8	-6.1
MRLC	- iPg	.997	111.1	127.5	-5.7
PTQR	+ iPg	1.02	113.23	310.3	-5.8
SGRT	+ iPg	1.05	116.57	67.9	-5.6
CDRU	- ePg	1.09	121.68	143.3	-5.4
FAGN	- ePg	1.10	122.69	324.7	-5.2
MSAG	+ iP*	1.15	128.08	72.1	22.8
CMPR	- eP*	1.24	137.36	148.0	22.8
CERT	- iP*	1.24	137.93	298.4	22.8
AQU	- iP*	1.25	139.58	322.1	22.8
PZUN	- eP*	1.26	139.95	124.7	22.8
ACER	+ iP*	1.27	141.55	116.8	22.8
RDP	- iPn	1.35	150.52	287.3	41.3
MRVN	+ iPn	1.35	150.82	102.6	41.3
RMP	- iPn	1.38	153.45	289.3	41.3
MA9	- iPn	1.39	155.53	287.3	41.3
CAMP	- iPn	1.40	155.55	326.9	41.3

Station	Polarity of first arrival	Epicentral distance, deg	Epicentral distance, km	Azimuth, deg	Incidence angle, deg
TERO	- iPn	1.40	155.79	333.8	41.3
MTCE	- iPn	1.43	159.34	297.8	41.3
MTSN	- iPn	1.48	164.85	137.7	41.3
MGR	- iPn	1.49	165.75	145.3	41.3
TRTR	+ iPn	1.49	165.82	344.9	41.3
SIRI	- iPn	1.60	178.39	137.3	41.3
MIGL	- ePn	1.69	188.28	116.2	41.3
CUC	- iPn	1.72	191.74	142.5	41.3
NRCA	- iPn	1.77	196.53	326.5	41.3
CESX	- iPn	1.86	206.52	312.5	41.3
FDMO	- iPn	1.95	216.55	329.4	41.3
TOLF	- iPn	1.95	217.68	291.7	41.3
CESI	- iPn	1.99	221.89	325.6	41.3
ARVD	- iPn	2.40	266.96	333.0	41.3
CELI	- iPn	2.52	280	140.7	41.3
ASQU	- iPn	3.12	346.91	322.0	41.3

Table 3

Parameters of focal mechanism for the event of 24.04.2011

Plane1			Plane2			P		T		N	
Strike (φ_s)	Dip (δ)	Slip (λ)	Strike (φ_s)	Dip (δ)	Slip (λ)	Azm	Plunge	Azm	Plunge	Azm	Plunge
192°	68°	30°	90°	63°	155°	320°	3°	52°	36°	226°	54°

Table 4

Parameters of focal mechanism for the event of 29.12.2013

Plane1			Plane2			P		T		N	
Strike (φ_s)	Dip (δ)	Slip (λ)	Strike (φ_s)	Dip (δ)	Slip (λ)	Azm	Plunge	Azm	Plunge	Azm	Plunge
316°	64°	-73°	102°	30°	-120°	257°	67°	33°	17°	129°	15°

References

1. Dziewonski A.M, Chou T.A.,Woodhouse J.H., (1981). Determination of earthquake source parameters from waveform data for studies of regional and global seismicity. *J.geophys.Res.*, 86, 2825-2852.

2. Godano M., Bardainne T., Regnier M., Deschamps A., (2011). Moment tensor determination by nonlinear inversion of amplitudes. *Bull.seism. Soc.Am.*, 101, 366-378.

3. Hardebeck J.L., Shearer P.M., (2003). Using S/P amplitude ratios to constrain the focal mechanisms of small earthquakes. *Bull.seism. Soc.Am.*, 93, 2432-2444.

4. Kikuchi M., Kanamori H., (1991). Inversion of complex body waves-III. *Bull.seism. Soc.Am.*, 81, 2335-2350.

5. Malytskyy D., Kozlovskyy E., (2014). Seismic waves in layered media. *J. of Earth Science and Engineering*, 4, 311-325.

6. Malytskyy D.V., (2010). Analytic-numerical approaches to the calculation of seismic moment tensor as a function of time. *Geoinformatika*, 1, 79-85. (In Ukrainian).

Малицький Д.В., (2010). Аналітично-числові підходи до обчислення часової залежності компонент тензора сейсмічного моменту. Геоінформатика, 1, 79-85.

7. Malytskyy D., Muyla O., Pavlova A., Hrytsaj O., (2013). Determining the focal mechanism of an earthquake in the Transcarpathian region of Ukraine. *Visnyk of Taras Shevchenko National University of Kyiv: Geology*, 4(63), 38-44.

8. Miller A.D., Julian B.R., Foulger G.R., (1998). Three-dimensional seismic structure and moment tensors of non-double-couple earthquakes at the Hengill-Grensdalur volcanic complex, Iceland. *Geophys. J. Int.*, 133, 309-325.

9. Sileny J., Panza G.F., Campus P., (1992). Waveform inversion for point source moment tensor retrieval with variable hypocentral depth and structural model. *Geophys. J. Int.*, 109, 259-274.

10. Sipkin S.A., (1986). Estimation of earthquake source parameters by the inversion of waveform data: Global seismicity, 1981-1983. *Bull.seism. Soc.Am.*, 76, 1515-1541.

11. Vavrychuk V., Kuhn D., (2012). Moment tensor inversion of waveforms: a two-step time frequency approach. *Geophys. J. Int.*, 190, 1761-1776.

Надійшла до редколегії 06.03.15

Д. Малицький, д-р фіз.-мат. наук, проф.
E-mail: dmytro@cb-igph.lviv.ua;
О. Муйла, канд. фіз.-мат. наук, мол. наук. співроб.
E-mail: orestaro@gmail.com;
О. Грицай, асп.
E-mail: grycaj.oksana@gmail.com;
О. Кутнів, інж. I кат.
E-mail: okutniv@yahoo.com;
О. Обідіна, асп.
E-mail: jane.det@yandex.ua;
Карпатське відділення Інституту геофізики ім. С.І. Субботіна НАН України,
вул. Наукова, 3-б, м. Львів, 79060 Україна

ВИЗНАЧЕННЯ ТЕНЗОРА СЕЙСМІЧНОГО МОМЕНТУ З ХВИЛЬОВИХ ФОРМ

Метою статті є визначення компонент тензора сейсмічного моменту та побудова механізму вогнища землетрусу з використанням записів сейсмічних станцій. У роботі застосовано матричний метод для побудови хвильового поля на вільній поверхні шаруватого середовища. Автори використовують методику виділення із повного хвильового поля частини, що відповідає поширенню прямих P та S хвиль. Визначення сейсмічного тензора як функції часу має велике практичне значення, оскільки дає можливість оцінити тривалість процесу утворення розриву, що генерує утворення сейсмічних хвиль. У результаті розв'язання оберненої задачі сейсмології, що зводиться до розв'язання системи матричних рівнянь, отримано часові залежності компонент тензора сейсмічного моменту. Результати розрахунків було апробовано на двох реальних сейсмічних подіях: у районі Мальти (24/04/2011, 13:02:12, 35.92°N, 14.95°E, MW=4.0) та Італії (29/12/2013, 17:09:0.04, 41.37°N, 14.45°E, MW=4.9), та проведено порівняльний аналіз з результатами, отриманими за допомогою графічного методу. Як результат досліджень було побудовано механізми вогнища даних землетрусів та визначено орієнтацію нодальних площин, а також час, протягом якого відбувалася подія. У роботі представлено теорію для визначення компонент тензора сейсмічного моменту як функцій часу у випадку реєстрації поля переміщень N станціями. Показано, що використання записів на одній станції може дати позитивний результат для визначення сейсмічного тензора й для побудови механізму вогнища землетрусу. У роботі використано нижню півсферу для побудови фокального механізму. Важливим для розв'язання оберненої задачі є точність задавання швидкісної моделі. На прикладі двох подій показано, що параметри та механізм вогнища для першої події визначено з більшою точністю, ніж для другої події. Показано, що для оберненої задачі з використанням хвильових форм є важливим визначення часів вступів прямих P та S хвиль та довжин їхніх записів. За значеннями перших максимумів на отриманих записах для компонент тензора сейсмічного моменту в результаті розв'язання оберненої задачі визначено механізми вогнищ землетрусів та параметри нодальних площин. Відзначено перспективи використання розподіленого джерела для розв'язування як прямих, так і обернених задач.

Ключові слова: матричний метод, часова функція джерела, механізм вогнища, тензор сейсмічного моменту.